





## Discovery of the Binarity of Gliese 229B, and Constraints on the System’s Properties

SAMUEL WHITEBOOK <sup>1,2</sup> TIMOTHY D. BRANDT <sup>3,1</sup> G. MIREK BRANDT <sup>1</sup> AND EMILY C. MARTIN <sup>4,5</sup>

<sup>1</sup>*Department of Physics, University of California, Santa Barbara, Santa Barbara, CA 93106, USA*

<sup>2</sup>*Division of Physics, Mathematics, and Astronomy, California Institute of Technology, Pasadena, CA 91125, USA*

<sup>3</sup>*Space Telescope Science Institute, 3700 San Martin Drive, Baltimore, MD 21218, USA*

<sup>4</sup>*Department of Astronomy and Astrophysics, University of California, Santa Cruz, Santa Cruz, CA, 95064, USA*

<sup>5</sup>*Planet Labs, PBC, San Francisco, CA, 94107, USA*

Submitted to ApJ Letters

### ABSTRACT

We present two epochs of radial velocities of the first imaged T dwarf Gliese 229 B obtained with Keck/NIRSPEC. The two radial velocities are discrepant with one another, and with the radial velocity of the host star, at  $\approx 11\sigma$  significance. This points to the existence of a previously postulated, but as-yet undetected, massive companion to Gl 229 B; we denote the two components as Gl 229 Ba and Gl 229 Bb. We compute the joint likelihood of the radial velocities to constrain the period and mass of the secondary companion. Our radial velocities are consistent with an orbital period between a few days and  $\approx 60$  days, and a secondary mass of at least  $\approx 15 M_{\text{Jup}}$  and up to nearly half the total system mass of Gl 229 B. With a significant fraction of the system mass in a faint companion, the strong tension between Gl 229 B’s dynamical mass and the predictions of evolutionary models is resolved.

#### Key words:

### 1. INTRODUCTION

Brown dwarfs lie below the minimum mass needed to achieve core hydrogen fusion (Burrows & Liebert 1993). Unable to reach the stellar main sequence, they cool and fade through spectral types M, L, T, and even Y (Kirkpatrick et al. 1999, 2012). These cooler spectral types are defined by the prominence of molecules like methane and CO in the atmosphere. Gl 229 B, discovered in 1995 (Nakajima et al. 1995; Oppenheimer et al. 1995), was the first unambiguously identified T dwarf; its methane-rich atmosphere was clear evidence that it was substellar.

Soon after its discovery, the first atmospheric and evolutionary analyses attempted to derive a mass and age for Gl 229 B from its observed spectrum and luminosity (Allard et al. 1996; Marley et al. 1996); these favored masses of  $\sim 30\text{--}50 M_{\text{Jup}}$ . A series of observations in the years following Gl 229 B’s discovery better established its infrared spectrum and even optical colors (Geballe et al. 1996; Golimowski et al. 1998; Oppenheimer et al. 1998; Leggett et al. 1999; Saumon et al. 2000). Under the first definition of the T spectral class

Gl 229B was classified as a T6.5V dwarf (Burrows et al. 2002), however it was later reclassified to a T7pec due to CH<sub>4</sub> features inconsistent with any standard T dwarf model (Burgasser et al. 2006). The volume of literature on Gl 229 B decreased in the years following its discovery as new data did not substantially change the initial atmospheric and evolutionary results.

Interest in Gl 229 B increased following the derivation of a surprisingly high dynamical mass of  $70.4 \pm 4.8 M_{\text{Jup}}$  (Brandt et al. 2020), in tension with all substellar evolutionary models. This dynamical mass relied on absolute astrometry cross-calibrated in the Hipparcos-Gaia Catalog of Accelerations (Brandt 2018, 2021) together with precision astrometry from the Hubble Space Telescope (Golimowski et al. 1998) and radial velocities (RVs) from the California Planet Survey (Butler et al. 2017). An updated analysis with better astrometry from the third Gaia data release (Lindgren et al. 2021; Brandt 2021) confirmed a mass of  $71.4 \pm 0.7 M_{\text{Jup}}$  for Gl 229 B (Brandt et al. 2021). At this mass, even 10 Gyr are insufficient for Gl 229 B to cool to its observed luminosity, while the properties of Gl 229 A suggest an age closer to  $\sim 1\text{--}3$  Gyr (Brandt et al. 2020). Brandt et al. (2020) and Brandt et al. (2021) both suggested that binarity could provide a solution: some of Gl 229 B’s mass could be held by an unseen

**Table 1.** Observing Log

Date (UT)	Target <sup>a</sup>	Band	$t_{\text{exp}}$ (s)	$N_{\text{exp}}$	$t_{\text{tot}}$ (s)
2022-03-12	Gl 229 B	<i>J</i>	300	7	2100
2022-03-12	Gl 229 B	<i>H</i>	300	5	1500
2022-03-12	Gl 229 B	<i>K</i>	300	4	1200
2022-11-10	Gl 229 A	<i>J</i>	15	4	60
2022-11-10	Gl 229 B	<i>J</i>	300	20	6000
2022-11-10	Gl 229 A	<i>H</i>	9	4	36
2022-11-10	Gl 229 B	<i>H</i>	300	8	2400
2022-11-10	Gl 229 A	<i>K</i>	15	4	60
2022-11-10	Gl 229 B	<i>K</i>	300	12	3600

<sup>a</sup>The 2022-03-12 data were taken without adaptive optics; speckles from Gl 229 A are visible in the slit. The 2022-11-10 data were taken with natural guide star adaptive optics.

companion, with the mass in the primary brown dwarf being consistent with expectations from the earlier evolutionary analyses.

Following the discovery of a surprisingly high mass for Gl 229 B, a number of retrievals have re-determined its properties, both with (Howe et al. 2023) and without (Calamari et al. 2022; Howe et al. 2022) the hypothesis of binarity. If the brown dwarf is single, it points to fundamental problems in substellar modeling. If Gl 229 B is a multiple, it indicates a complex dynamical structure for the first brown dwarf system to be imaged, and could present new tests for evolutionary models. Gl 229 Ba and a hypothetical Gl 229 Bb would have the same age and composition, and with precise individual masses, they could enable rare consistency tests of evolutionary models that are possible for a handful of systems (Dupuy et al. 2015; Chen et al. 2022).

In this paper we present two epochs of new spectroscopic observations of Gl 229 B to measure its RV. This can be used to test for additional motion beyond the orbit of the system around its host star, and thereby test for binary, and ultimately measure the individual masses and orbit. We organize the paper as follows: Section 2 covers the reduction of spectra taken from KECK/NIRSPEC. In Section 3 we discuss the measurement of RVs by shifting observations against model spectra. Sections 4 and 5 discuss parameters derived from the measured RV anomalies and the status of the Gl 229 B system.

## 2. OBSERVATIONS AND DATA REDUCTION

We obtained spectra of Gl 229B using Keck/NIRSPEC (McLean et al. 1998) on March 12, 2022 and November 10, 2022 UT in high resolution mode ( $R \sim 25000$ ) in the *J*,

*H*, and *K* bands spanning wavelengths from 1.128 - 2.771  $\mu\text{m}$ . For the March 2022 data, we used NIRSPEC in natural seeing mode with the 0''.432 slit, while for the November 2022 data we used natural guide star adaptive optics (NIRSPA0) with the 0''.041 slit. For the latter date we obtained spectra of Gl 229A with short exposure times followed by spectra of Gl 229B with long exposure times. Table 1 lists our observing log. Both epochs used an ABBA nod pattern.

All data were reduced using a custom pipeline. We removed amplifier glow and/or a reset anomaly by fitting an exponential to the lowest 100 rows of each column. Spectral orders were cut out by finding the locations of wavelength orders in flat lamps and then rectified by a transformation matrix that linearized the stellar trace along the dispersion direction and minimized the variance of the arc lamp row sums perpendicular to it. In order to avoid the impact of dead and hot pixels, we utilized the Gaussian process regression module *astrofix* (Zhang & Brandt 2021) to impute their values. Post-rectification pixels that had more than a 10% contribution from bad pixels were then masked and weighted to zero during extraction later. Spectra were extracted using the optimal extraction algorithm described in Horne (1986); the profiles of the traces were obtained from Gaussian fits to the median of the traces along the dispersion direction. Bad pixel masks were created individually for each exposure. Dead and hot pixels were masked from the pre-rectification dark images. We also masked  $>3\sigma$  outliers in each exposure, with  $\sigma$  robustly estimated from the surrounding  $7 \times 7$  pixels by 1.48 times the median absolute deviation. Extracted spectra were further cleaned by Fourier transforming the spectra, setting Fourier modes corrupted by fringing from the detector to zero, and then inverting the Fourier transform. These modes are much lower in spatial frequency than the lines used to determine RVs. The blaze function of each spectrum was found by fitting a 5th degree polynomial to the observed spectrum and subsequently divided out.

Data taken in March (with natural seeing) had significant diffraction from Gl 229 A resulting in speckle traces overlapping the spectrum of Gl 229 B. This left two usable orders with  $\text{SNR} > 10$ : orders 58 and 59 in *J* band. Traces representing diffraction speckles of Gl 229 A were modeled by Gaussian kernels along the spatial dimension and removed before extracting the spectrum of Gl 229 B. We computed our wavelength solution in the March data using OH sky lines. As explained in Section 3, we recover the accepted RV of Gl 229 A from diffracted starlight in the March data.

Our November data were taken using natural guide star adaptive optics (AO) (Wizinowich et al. 2000) to mitigate the effects of stellar diffraction by enabling the use of a smaller slit. Because the smaller slit and PSF greatly reduce the relative strength of sky lines, wavelength solutions in AO data were found by fitting Gaussians to observed ArNeXeKr arc

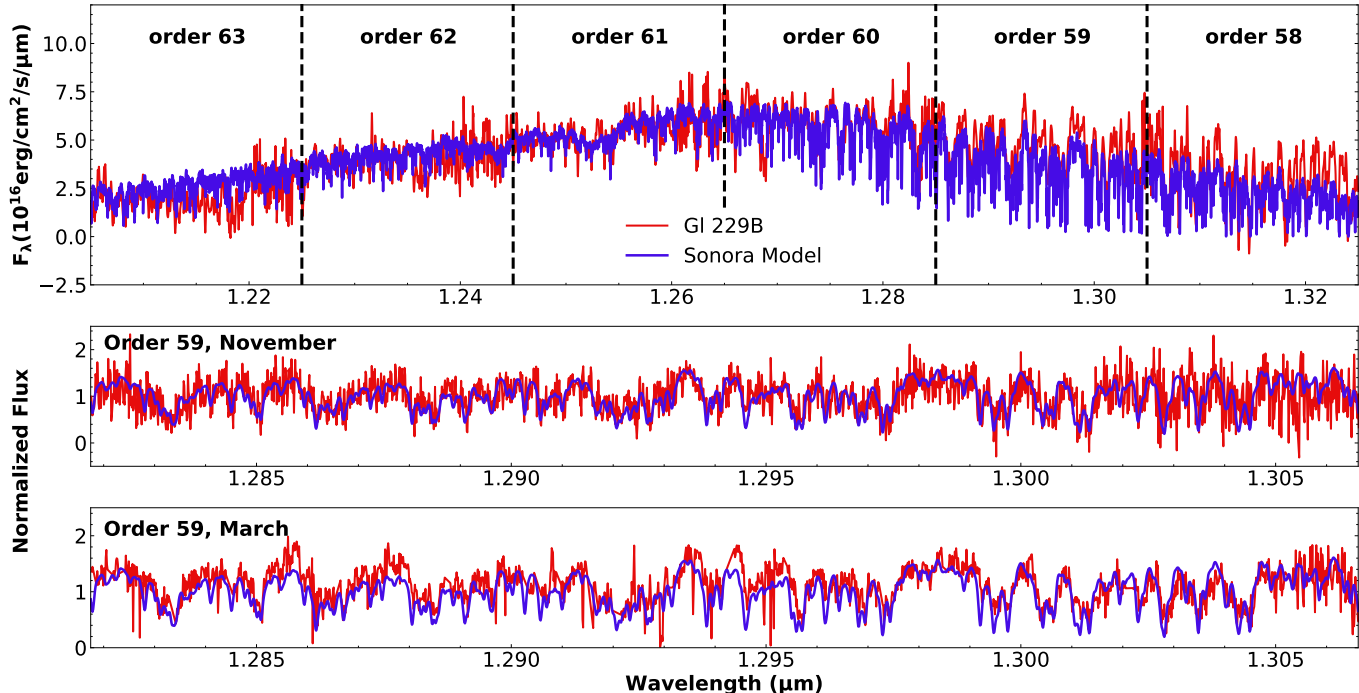


**Figure 1.** Top: The spectrum of Gliese 229B in the  $J$  band between orders 58 and 63 taken in November 2022. The spectrum is flux-calibrated by a sensitivity function derived from Gl 229A and convolved to a resolution of  $R \sim 8000$ . A Sonora model (Marley et al. 2021) with  $T = 850$  K and  $\log_{10}(g/\text{cm s}^{-2}) = 5.0$  is overlaid. Middle: The highest resolution  $R \sim 25000$  spectrum of Gl 229B from order 59 normalized and shifted to the solar system barycenter rest frame versus the normalized Sonora model. Bottom: The same full-resolution order 59 spectrum as the middle panel, but for the natural seeing data from March 2022.

lamp lines and then fitting a polynomial transformation between the centers of these Gaussians and catalogued points provided by the Keck Observatory (McLean et al. 1998). We calculate the root-mean-square deviation (RMSD) of the residuals between the fitted and tabulated line locations and discard orders with  $\text{RMSD} > 0.1 \text{ \AA}$  (including order 58, which we used in the March data). After these initial data cuts we retain 14 orders. We further cut the November data to only consider orders with  $\text{SNR} > 10$ , leaving just three orders: order 47 in  $H$  band and orders 59 and 60 in  $J$  band. Telluric corrections in November were derived directly by dividing the observed spectra of Gl 229A by model spectra.

### 3. RADIAL VELOCITY ANOMALY DETECTION

Gl 229B has a well-determined orbit (Brandt 2021). Using the python package REBOUND (Rein & Liu 2012), we predict an RV of  $0 \pm 300 \text{ m s}^{-1}$  for Gl 229B relative to Gl 229A in both March and November of 2022 (Figure 2) where  $300 \text{ m s}^{-1}$  is  $1\sigma$  of the (nearly Gaussian) distribution of derived orbits. This is the relative RV of the barycenters of Gl 229 A and B, and will be the same as the relative RV of the two objects if Gl 229 B is singular. The predicted RV change of a singular Gl 229B across 2022 is very low,  $\approx 1 \text{ m s}^{-1}$ .

The actual RVs of both Gl 229A and Gl 229B were calculated by finding the redshift that minimizes  $\chi^2$  between the observed spectra and relevant rest frame models. The

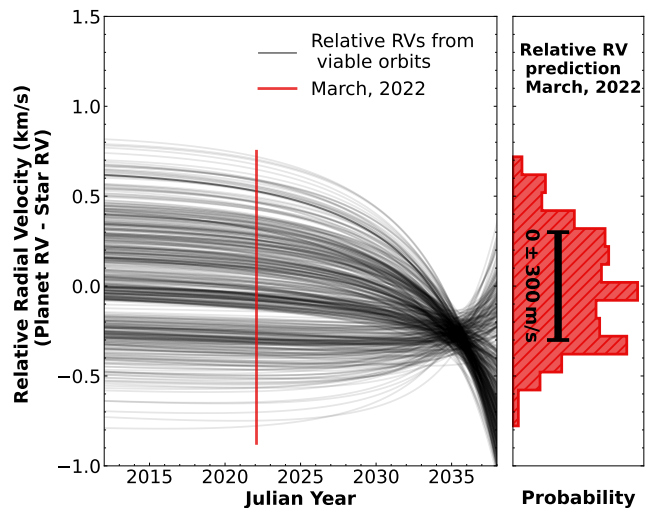


**Figure 2.** The relative radial velocity of Gl 229B (The RV of Gl 229B minus that of Gl 229A) if the BD is singular. The orbits are drawn from the posterior in Brandt et al. (2021).

error used in  $\chi^2$  fitting is derived from Poisson statistics. We take the blaze function to be the photon count at every wavelength. The spectra are normalized for fitting against the blaze function, so the variance on the measured spectra is  $\sigma^2(\lambda) = 1/F(\lambda)$  where  $F(\lambda)$  is the blaze function. Additionally, a telluric model derived from Noll et al. (2012) is used to

impart an additional uncertainty added in quadrature to each wavelength bin in correspondence with its absorption.

GI 229A was modeled using a high resolution M dwarf spectrum generated by the stellar atmosphere code PHOENIX (Husser et al. 2013) with  $T_{\text{eff}} = 3700$  K and  $\log(g) = 4.50$  (cgs) parameters chosen to roughly match GI 229A. GI 229B was modeled using the Sonora BD atmosphere models (Marley et al. 2021) with  $T_{\text{eff}} = 850$  K,  $\log(g) = 5.0$  (cgs). Each order’s model spectrum was normalized by dividing out the best fit first degree polynomial continuum over the wavelength range of the spectral order. This puts the model and the observed spectrum in the same arbitrary unit basis.

Radial velocities calculated by  $\chi^2$  were barycenter corrected using the python package `barycorrpy` (Kanodia & Wright 2018). The November spectra of GI 229B were taken over the span of approximately 3 hours for *J* band, and approximately 1 hour for *H* and *K* bands, and then averaged; spectra of the brown dwarf were barycenter corrected with respect to the mean observation time of each band. We derive uncertainties by bootstrap resampling, or redrawing data with replacement many times (Efron 1979), the individual exposures used to derive RVs. Using `barycorrpy` we find that the rotation of the Earth over the observational time frame imparts an additional uncertainty of  $\approx 105$  m s $^{-1}$  on the measured RV of GI 229B; we add this uncertainty in quadrature. GI 229 A is not subject to this uncertainty, as only a single 30 second exposure of the M dwarf was used.

Spectra of GI 229 A were not taken in March. Instead, the RV of the star was derived from diffracted starlight in exposures of GI 229 B. From the speckle traces of GI 229 A in the natural seeing data, we derive an RV of  $3.3 \pm 1.4$  km s $^{-1}$  for the star in March. This uncertainty is derived from  $\Delta\chi^2 = 1$  and may be less reliable than the one derived using bootstrap resampling of the November data, for which we derive an RV of  $3.18 \pm 0.36$  km s $^{-1}$ . However, our March RV of GI 229A agrees well with both our November measurement and with RVs derived in the literature (e.g.,  $4.7$  km s $^{-1}$  from Nidever et al. (2002) and  $4.2$  km s $^{-1}$  from Gaia (Gaia Collaboration et al. 2023)). Thus, for the purpose of reporting discrepancies in the theoretical relative RV of the system, we compare the RV of GI 229 B in both epochs to the RV of GI 229 A in November.

We report a radial velocity difference of  $-10.35 \pm 0.71$  km s $^{-1}$  between GI 229A and 229B in March 2022, and a difference of  $2.74 \pm 1.09$  km s $^{-1}$  in November. These RVs are  $14.5\sigma$  and  $2.5\sigma$  discrepant, respectively, with the difference of  $0 \pm 300$  m s $^{-1}$  expected from the system’s known orbit.

#### 4. CONSTRAINTS ON THE SUBCOMPANION

Figure 3 shows our two RV measurements of GI 229 B together with our measured RV of GI 229 A. The RV of GI 229 A is known to be stable at the several m/s level over

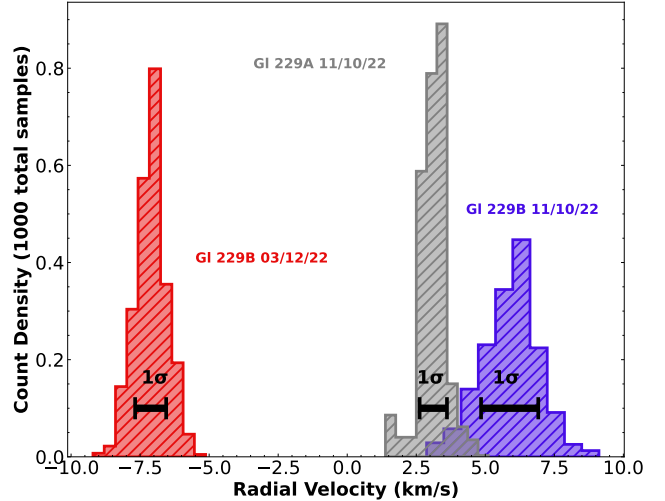


**Figure 3.** Distributions of individual component RVs in both observation epochs derived from bootstrap resampled spectra. Diffracted spectra of GI 229 A in March provide a consistent but less precise RV, so both epochs of GI 229 B RVs are compared to that of GI 229 A from November. The RV of the GI 229 B system varies by more than  $11\sigma$  between observations, completely ruling out singularity.

a period of a year (Tuomi et al. 2014), orders of magnitude better than our precision. The March 2022 RV of GI 229 B differs from the prediction for the barycenter motion of its orbit by nearly  $15\sigma$ , ruling out GI 229 B’s status as a single object. We now proceed to use our two RVs to constrain the properties of the GI 229 B system: its orbital period, and the mass of the less massive component, which we denote GI 229 Bb.

We measure the likelihood of a mass for GI 229 Bb and an orbital period of the system assuming a random orbital phase and orientation, and a uniform distribution of eccentricity up to 0.8. High eccentricities are common in stellar binaries until tidal circularization damps them (e.g. Meibom & Mathieu 2005; Geller et al. 2021). Periods of  $\leq 10$  days are circularized for stars at ages of a few Gyr (Meibom & Mathieu 2005; Geller et al. 2021), but the much smaller sizes of brown dwarfs will reduce the efficiency of tidal damping and allow eccentric orbits to remain so down to shorter periods. The eclipsing M dwarf-brown dwarf binary TOI-2119, for example, has an eccentricity  $\approx 0.3$  despite a period of just  $\approx 7$  days (Cañas et al. 2022). We adopt a lower limit on the orbital period of 1 day, which would correspond to a semimajor axis of about  $1.6 R_{\odot}$ . We adopt an upper limit of  $35 M_{\text{Jup}}$  on the mass of GI 229 Bb, as the secondary should be less massive than the primary in order to have a lower luminosity. We do not account for any dependence of the eccentricity on the orbital period; this is a secondary effect on the resulting probability distributions of RVs given the narrow range of periods, from one to a few days, over which tidal circularization could be efficient.



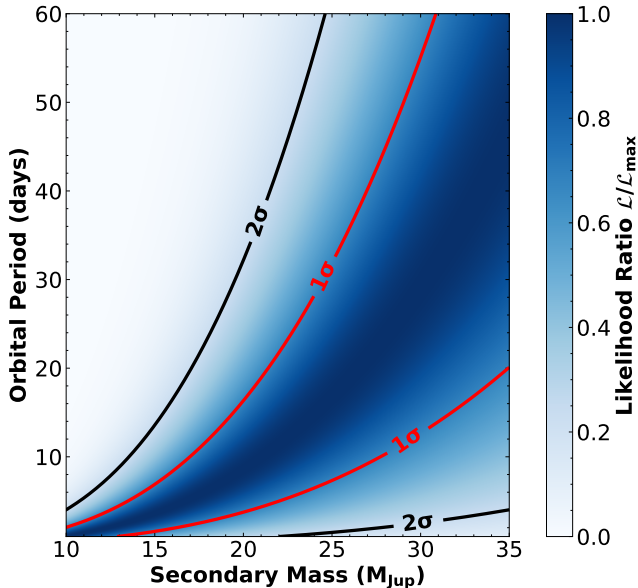


**Figure 4.** Joint likelihood of orbital period and mass of Gl 229 Bb given our two RV measurements, assuming random eccentricities between 0 and 0.8, random orbital phases and orientations, and a minimum period of 1 day (corresponding to a minimum semimajor axis of  $\approx 1.6 R_{\odot}$ ). Our two RV measurements confirm that at least  $\approx 15 M_{\text{Jup}}$  of the Gl 229 B system reside in Gl 229 Bb.

We use a grid of points in orbital phase and argument of periastron to compute a probability distribution of observing the system at a given fraction of its RV semiamplitude. These probability distributions depend on eccentricity, while the RV semiamplitude depends on companion mass, period and inclination (the total mass of the Gl 229 B system is accurately known). We then multiply the probability distributions of RV by the two observational probability distributions, integrate each of these products, and multiply the two results to obtain a likelihood of a given eccentricity, orbital period, and mass of Gl 229 Bb. Finally, we marginalize these distributions over eccentricity.

Figure 4 shows our results. We obtain a mass of Gl 229 Bb of at least  $\approx 15 M_{\text{Jup}}$ , with values up to half of the system mass being entirely consistent with the RV data. Given that Gl 229 Bb should be the less massive body in the system, we constrain the orbital period of the binary to be  $\lesssim 120$  days at  $2\sigma$  and at the highest possible mass of Gl 229 Bb, and  $\lesssim 50$  days at  $1\sigma$  assuming the mass ratio between Gl 229 Ba and Gl 229 Bb to be at least somewhat less than unity. This constraint establishes Gl 229 Bb as the unseen reservoir for a substantial fraction of Gl 229 B’s mass.

Our RV orbital constraints at the longer allowable periods are in mild tension with the results of Brandt et al. (2020) and Brandt (2021). Those authors disfavored an orbital semimajor axis of Gl 229 Ba of more than a few mas based on the excellent agreement between Hubble Space Telescope rela-

tive astrometry and an orbital fit with Gl 229 B as a single object. This qualitative upper limit on semimajor axis is a few 0.01 au at the distance to Gl 229, corresponding to an orbital period of a few days assuming a mass ratio close to unity. The HST observations came in several pairs separated by about six months, so these loose constraints could be evaded depending on the exact orbital period, the alignment of the system, and the possible contribution of Gl 229 Bb to the system’s luminosity in the bands observed by Hubble. However, they do favor periods and masses toward the shorter end of our allowable space,  $\sim 20 M_{\text{Jup}}$  at a period of  $\lesssim 1$  week. This would leave Gl 229 Ba as a  $\sim 50 M_{\text{Jup}}$  object, removing the strong tension between the dynamical mass and substellar cooling models (Brandt et al. 2021).

Finally, we look for direct spectral evidence of Gl 229 Bb. At an age of  $\lesssim 3$  Gyr (Brandt et al. 2020) and a mass  $\gtrsim 15 M_{\text{Jup}}$ , Gl 229 Bb would have an effective temperature of at least  $\approx 450$  K (Phillips et al. 2020), corresponding to a spectral type no later than early Y. Assuming the same radius for both objects, we fit the sum of two model atmospheres at different temperatures to our observed spectra, but find no pair of temperatures to provide a consistently better fit across spectral orders than a single temperature model.

## 5. DISCUSSION AND CONCLUSION

Models of substellar evolution couple a fully convective interior to an atmosphere with complex chemistry, molecules, and clouds (Burrows et al. 1997; Allard et al. 2001). These models, initially used to infer masses and ages from observed spectra and luminosities (e.g. Allard et al. 1996; McCaughrean et al. 2004), can now be tested with the aid of dynamical mass measurements and ages from the host stars of substellar companions (Dupuy & Liu 2017).

Several late T dwarf companions to main sequence stars have recently been found to have very high masses, close to the stellar/substellar boundary. WISE J0720-0846B, with a mass of  $66 \pm 4 M_{\text{Jup}}$  (Dupuy et al. 2019), can be reconciled with substellar models assuming an old age for the system.  $\varepsilon$  Indi C, at  $70.1 \pm 0.7 M_{\text{Jup}}$  (Dieterich et al. 2018), is difficult to reconcile with substellar cooling models at any age. However, a subsequent dynamical analysis with much more data found a lower mass of  $53.25 \pm 0.29 M_{\text{Jup}}$ , fully consistent with cooling models (Chen et al. 2022). Two more late T dwarf companions, HD 4113 C and Gl 229 B, appear much too massive to have cooled to their low observed luminosities (Cheetham et al. 2018; Brandt et al. 2021). Two possible explanations for these high dynamical masses are incorrect mass measurements or faint binary companions holding a substantial amount of mass. The alternative is a serious failure of substellar evolutionary modeling. Gl 229 B has a  $>100\sigma$  acceleration between Hipparcos and Gaia (Brandt 2021), making unresolved binarity an especially attractive so-

lution despite the fact that field T dwarfs show a low binary fraction (Fontanive et al. 2018).

This paper presents conclusive evidence that Gl 229 B is, in fact, an unresolved binary. Using two epochs of NIRSPEC spectroscopy on Keck, we find that Gl 229 B's RV varies from that expected from its orbit by  $2.7 \text{ km s}^{-1}$  and by  $10.4 \text{ km s}^{-1}$ . These values differ from one another and from the RV of the host star by  $\approx 11\sigma$ . With only two epochs, we cannot derive a full orbital solution, but we can place important constraints on the properties of the system.

We find that the unseen companion, which we designate Gl 229 Bb, is at least  $\approx 15 M_{\text{Jup}}$ , and could be nearly as massive as Gl 229 Ba. The highest portion of this range is disfavored by existing Hubble Space Telescope astrometry that does not show Gl 229 B deviating from the orbit expected of its barycenter. However, with the limited nature of these data and the range of orientations the Gl 229 B system could

have, we cannot fully rule out such high companion masses. We find that the orbital period of the system is no more than  $\approx 100$  days and likely significantly less. Future RV monitoring will be able to derive a precise orbit and individual masses for the two components in the Gl 229 B system. If more T dwarf companions to main sequence stars are discovered to host companions, it may point to a higher multiplicity fraction in brown dwarf companions than in the field (Fontanive et al. 2018).

With at least  $\approx 15 M_{\text{Jup}}$  of the Gl 229 B system in Gl 229 Bb, the tension between Gl 229 Ba's dynamical mass and the predictions of substellar evolutionary models is mostly or entirely resolved. Gl 229 B then stands as an example of substellar binarity, a constraint on substellar formation mechanisms, and potentially a system for which two coeval substellar objects can both have their ages, masses, spectra, and luminosities measured.

## REFERENCES

- Allard, F., Hauschildt, P. H., Alexander, D. R., Tamanai, A., & Schweitzer, A. 2001, *ApJ*, 556, 357, doi: [10.1086/321547](https://doi.org/10.1086/321547)
- Allard, F., Hauschildt, P. H., Baraffe, I., & Chabrier, G. 1996, *ApJL*, 465, L123, doi: [10.1086/310143](https://doi.org/10.1086/310143)
- Brandt, G. M., Dupuy, T. J., Li, Y., et al. 2021, *AJ*, 162, 301, doi: [10.3847/1538-3881/ac273e](https://doi.org/10.3847/1538-3881/ac273e)
- Brandt, T. D. 2018, *ApJS*, 239, 31, doi: [10.3847/1538-4365/aaec06](https://doi.org/10.3847/1538-4365/aaec06)
- , 2021, *ApJS*, 254, 42, doi: [10.3847/1538-4365/abf93c](https://doi.org/10.3847/1538-4365/abf93c)
- Brandt, T. D., Dupuy, T. J., Bowler, B. P., et al. 2020, *AJ*, 160, 196, doi: [10.3847/1538-3881/abb45e](https://doi.org/10.3847/1538-3881/abb45e)
- Burgasser, A. J., Geballe, T. R., Leggett, S. K., Kirkpatrick, J. D., & Golimowski, D. A. 2006, *ApJ*, 637, 1067, doi: [10.1086/498563](https://doi.org/10.1086/498563)
- Burrows, A., Burgasser, A. J., Kirkpatrick, J. D., et al. 2002, *ApJ*, 573, 394, doi: [10.1086/340584](https://doi.org/10.1086/340584)
- Burrows, A., & Liebert, J. 1993, *Reviews of Modern Physics*, 65, 301, doi: [10.1103/RevModPhys.65.301](https://doi.org/10.1103/RevModPhys.65.301)
- Burrows, A., Marley, M., Hubbard, W. B., et al. 1997, *ApJ*, 491, 856, doi: [10.1086/305002](https://doi.org/10.1086/305002)
- Butler, R. P., Vogt, S. S., Laughlin, G., et al. 2017, *AJ*, 153, 208, doi: [10.3847/1538-3881/aa66ca](https://doi.org/10.3847/1538-3881/aa66ca)
- Cañas, C. I., Mahadevan, S., Bender, C. F., et al. 2022, *AJ*, 163, 89, doi: [10.3847/1538-3881/ac415f](https://doi.org/10.3847/1538-3881/ac415f)
- Calamari, E., Faherty, J. K., Burningham, B., et al. 2022, *ApJ*, 940, 164, doi: [10.3847/1538-4357/ac9cc9](https://doi.org/10.3847/1538-4357/ac9cc9)
- Cheetham, A., Ségransan, D., Peretti, S., et al. 2018, *A&A*, 614, A16, doi: [10.1051/0004-6361/201630136](https://doi.org/10.1051/0004-6361/201630136)
- Chen, M., Li, Y., Brandt, T. D., et al. 2022, *AJ*, 163, 288, doi: [10.3847/1538-3881/ac66d2](https://doi.org/10.3847/1538-3881/ac66d2)
- Dieterich, S. B., Weinberger, A. J., Boss, A. P., et al. 2018, *ApJ*, 865, 28, doi: [10.3847/1538-4357/aadadc](https://doi.org/10.3847/1538-4357/aadadc)
- Dupuy, T. J., & Liu, M. C. 2017, *ApJS*, 231, 15, doi: [10.3847/1538-4365/aa5e4c](https://doi.org/10.3847/1538-4365/aa5e4c)
- Dupuy, T. J., Liu, M. C., Leggett, S. K., et al. 2015, *ApJ*, 805, 56, doi: [10.1088/0004-637X/805/1/56](https://doi.org/10.1088/0004-637X/805/1/56)
- Dupuy, T. J., Liu, M. C., Best, W. M. J., et al. 2019, *AJ*, 158, 174, doi: [10.3847/1538-3881/ab3cd1](https://doi.org/10.3847/1538-3881/ab3cd1)
- Efron, B. 1979, *The Annals of Statistics*, 7, 1, doi: [10.1214/aos/1176344552](https://doi.org/10.1214/aos/1176344552)
- Fontanive, C., Biller, B., Bonavita, M., & Allers, K. 2018, *MNRAS*, 479, 2702, doi: [10.1093/mnras/sty1682](https://doi.org/10.1093/mnras/sty1682)
- Gaia Collaboration, Vallenari, A., Brown, A. G. A., et al. 2023, *A&A*, 674, A1, doi: [10.1051/0004-6361/202243940](https://doi.org/10.1051/0004-6361/202243940)
- Geballe, T. R., Kulkarni, S. R., Woodward, C. E., & Sloan, G. C. 1996, *ApJL*, 467, L101, doi: [10.1086/310203](https://doi.org/10.1086/310203)
- Geller, A. M., Mathieu, R. D., Latham, D. W., et al. 2021, *AJ*, 161, 190, doi: [10.3847/1538-3881/abdd23](https://doi.org/10.3847/1538-3881/abdd23)
- Golimowski, D. A., Burrows, C. J., Kulkarni, S. R., Oppenheimer, B. R., & Bruckardt, R. A. 1998, *AJ*, 115, 2579, doi: [10.1086/300370](https://doi.org/10.1086/300370)
- Horne, K. 1986, *PASP*, 98, 609, doi: [10.1086/131801](https://doi.org/10.1086/131801)
- Howe, A. R., Mandell, A. M., & McElwain, M. W. 2023, *ApJL*, 951, L25, doi: [10.3847/2041-8213/acdd76](https://doi.org/10.3847/2041-8213/acdd76)
- Howe, A. R., McElwain, M. W., & Mandell, A. M. 2022, *ApJ*, 935, 107, doi: [10.3847/1538-4357/ac5590](https://doi.org/10.3847/1538-4357/ac5590)
- Husser, T. O., Wende-von Berg, S., Dreizler, S., et al. 2013, *A&A*, 553, A6, doi: [10.1051/0004-6361/201219058](https://doi.org/10.1051/0004-6361/201219058)
- Kanodia, S., & Wright, J. 2018, *Research Notes of the American Astronomical Society*, 2, 4, doi: [10.3847/2515-5172/aaa4b7](https://doi.org/10.3847/2515-5172/aaa4b7)
- Kirkpatrick, J. D., Reid, I. N., Liebert, J., et al. 1999, *ApJ*, 519, 802, doi: [10.1086/307414](https://doi.org/10.1086/307414)

- Kirkpatrick, J. D., Gelino, C. R., Cushing, M. C., et al. 2012, *ApJ*, 753, 156, doi: [10.1088/0004-637X/753/2/156](https://doi.org/10.1088/0004-637X/753/2/156)
- Leggett, S. K., Toomey, D. W., Geballe, T. R., & Brown, R. H. 1999, *ApJL*, 517, L139, doi: [10.1086/312049](https://doi.org/10.1086/312049)
- Lindgren, L., Klioner, S. A., Hernández, J., et al. 2021, *A&A*, 649, A2, doi: [10.1051/0004-6361/202039709](https://doi.org/10.1051/0004-6361/202039709)
- Marley, M. S., Saumon, D., Guillot, T., et al. 1996, *Science*, 272, 1919, doi: [10.1126/science.272.5270.1919](https://doi.org/10.1126/science.272.5270.1919)
- Marley, M. S., Saumon, D., Visscher, C., et al. 2021, *ApJ*, 920, 85, doi: [10.3847/1538-4357/ac141d](https://doi.org/10.3847/1538-4357/ac141d)
- McCaughrean, M. J., Close, L. M., Scholz, R. D., et al. 2004, *A&A*, 413, 1029, doi: [10.1051/0004-6361:20034292](https://doi.org/10.1051/0004-6361:20034292)
- McLean, I. S., Becklin, E. E., Bendiksen, O., et al. 1998, in *Society of Photo-Optical Instrumentation Engineers (SPIE) Conference Series*, Vol. 3354, *Infrared Astronomical Instrumentation*, ed. A. M. Fowler, 566–578, doi: [10.1117/12.317283](https://doi.org/10.1117/12.317283)
- Meibom, S., & Mathieu, R. D. 2005, *ApJ*, 620, 970, doi: [10.1086/427082](https://doi.org/10.1086/427082)
- Nakajima, T., Oppenheimer, B. R., Kulkarni, S. R., et al. 1995, *Nature*, 378, 463, doi: [10.1038/378463a0](https://doi.org/10.1038/378463a0)
- Nidever, D. L., Marcy, G. W., Butler, R. P., Fischer, D. A., & Vogt, S. S. 2002, *ApJS*, 141, 503, doi: [10.1086/340570](https://doi.org/10.1086/340570)
- Noll, S., Kausch, W., Barden, M., et al. 2012, *A&A*, 543, A92, doi: [10.1051/0004-6361/201219040](https://doi.org/10.1051/0004-6361/201219040)
- Oppenheimer, B. R., Kulkarni, S. R., Matthews, K., & Nakajima, T. 1995, *Science*, 270, 1478, doi: [10.1126/science.270.5241.1478](https://doi.org/10.1126/science.270.5241.1478)
- Oppenheimer, B. R., Kulkarni, S. R., Matthews, K., & van Kerkwijk, M. H. 1998, *ApJ*, 502, 932, doi: [10.1086/305928](https://doi.org/10.1086/305928)
- Phillips, M. W., Tremblin, P., Baraffe, I., et al. 2020, *A&A*, 637, A38, doi: [10.1051/0004-6361/201937381](https://doi.org/10.1051/0004-6361/201937381)
- Rein, H., & Liu, S. F. 2012, *A&A*, 537, A128, doi: [10.1051/0004-6361/201118085](https://doi.org/10.1051/0004-6361/201118085)
- Saumon, D., Geballe, T. R., Leggett, S. K., et al. 2000, *ApJ*, 541, 374, doi: [10.1086/309410](https://doi.org/10.1086/309410)
- Tuomi, M., Jones, H. R. A., Barnes, J. R., Anglada-Escudé, G., & Jenkins, J. S. 2014, *MNRAS*, 441, 1545, doi: [10.1093/mnras/stu358](https://doi.org/10.1093/mnras/stu358)
- Wizinowich, P., Acton, D. S., Shelton, C., et al. 2000, *PASP*, 112, 315, doi: [10.1086/316543](https://doi.org/10.1086/316543)
- Zhang, H., & Brandt, T. D. 2021, *AJ*, 162, 139, doi: [10.3847/1538-3881/ac1348](https://doi.org/10.3847/1538-3881/ac1348)